Oncogenic steroid receptor coactivator-3 is a key regulator of the white adipogenic program

Jean-Francois Louet*, Agnès Coste†, Larbi Amazit*, Mounia Tannour-Louet‡, Ray-Chang Wu*, Sophia Y. Tsai*, Ming-Jer Tsai*, Johan Auwerx†§, and Bert W. O'Malley*¶

Departments of *Molecular and Cellular Biology and ‡Obstetrics and Gynecology, Baylor College of Medicine, One Baylor Plaza, Houston, TX 77030; †Institut de Génétique et de Biologie Moléculaire et Cellulaire, Centre National de la Recherche Scientifique, Institut National de la Santé et de la Recherche Médicale, Université Louis Pasteur, 67404 Illkirch, France; and §Institut Clinique de la Souris, Génopole Strasbourg, 67404 Illkirch, France

Contributed by Bert W. O'Malley, October 2, 2006 (sent for review September 7, 2006)

The white adipocyte is at the center of dysfunctional regulatory pathways in various pathophysiological processes, including obesity, diabetes, inflammation, and cancer. Here, we show that the oncogenic steroid receptor coactivator-3 (SRC-3) is a critical regulator of white adipocyte development. Indeed, in *SRC-3*$^{-/-}$ mouse embryonic fibroblasts, adipocyte differentiation was severely impaired, and reexpression of SRC-3 was able to restore it. The early stages of adipocyte differentiation are accompanied by an increase in nuclear levels of SRC-3, which accumulates to high levels specifically in the nucleus of differentiated fat cells. Moreover, *SRC-3*$^{-/-}$ animals showed reduced body weight and adipose tissue mass with a significant decrease of the expression of peroxisome proliferator-activated receptor γ2 (PPARγ2), a master gene required for adipogenesis. At the molecular level, SRC-3 acts synergistically with the transcription factor CAAT/enhancer-binding protein to control the gene expression of PPARγ2. Collectively, these data suggest a crucial role for SRC-3 as an integrator of the complex transcriptional network controlling adipogenesis.

adipogenesis | peroxisome proliferator-activated receptor (PPAR) | transcription | coregulators | metabolism

Obesity is one of the most common nutritional disorders in the developed world, and it is closely associated with important syndromes including type 2 diabetes, hypertension, coronary heart disease, osteoarthritis, and cancer. Obesity is clinically characterized by increased white adipose tissue (WAT) mass that results from both increased fat-cell size and increased fat-cell number (1). The number of adipocytes present in the organism is determined to a large degree by the adipocyte-differentiation process, which generates mature adipocytes from fibroblast-like preadipocytes. The adipogenic program is controlled by an array of interacting transcription factors operating to coordinate expression of hundreds of proteins that give rise to mature endocrine fat cells. Selected nuclear receptors have been reported to be involved in the complex network of transcription factors driving adipocyte differentiation (2). In particular, peroxisome proliferator-activated receptor γ (PPARγ), in association with its binding partner retinoid X receptor α, functions as a master regulator of adipocyte differentiation (3).

Because coregulators mediate the functions of nuclear receptors, they are likely coordinators for the efficient expression of gene sets controlling adipogenesis. However, the impact of coregulators remains less explored in adipose tissue biology. From recent studies, it appears that in addition to PPARγ coactivator-1 family members, the most studied coregulators in the field of metabolism, additional cofactors act along with these coactivators to influence energy balance and adipogenesis (4, 5).

Steroid receptor coactivator-3 (SRC-3), a member of the p160 family of nuclear receptor coactivators, is frequently amplified and overexpressed in breast cancers (6). This coactivator is known to play important roles in multiple physiological processes, including mammary gland development, cell proliferation, somatic growth, female reproductive function, puberty, cytokine signaling, vasoprotection, and lymphopoiesis (7). Depending on the cellular and molecular context, SRC-3 has been described as an oncogene because its overexpression in mice leads to the development of mammary gland tumors (8). Conversely, in the lymphoid system, it acts as a tumor suppressor, as evidenced by the development of lymphomas in *SRC-3*$^{-/-}$ mice (9).

Based on the important biological activity of SRC-3 and according to the emergent and promising role of coregulators in metabolic pathways (10), the impact of SRC-3 on adipogenesis has been investigated in this work. *SRC-3*$^{-/-}$ mice present a significant reduction in fat mass under basal conditions. This lean phenotype of *SRC-3*$^{-/-}$ mice is linked to impaired white adipocyte differentiation. At the molecular level, SRC-3 acts synergistically with CAAT/enhancer-binding protein (C/EBP) to control the gene expression of PPARγ2, the master transcription factor required for adipocyte differentiation. Taken together, our findings uncovered a crucial role of the coactivator SRC-3 in the complex transcriptional network controlling the adipogenic program.

Results

Adipogenesis Is Severely Impaired in the Absence of SRC-3, and Ectopic Reexpression of SRC-3 Restores the Adipogenic Program. We first explored the specific action of SRC-3 on the adipocyte differentiation process *per se* by using mouse embryonic fibroblasts (MEFs), isolated from *SRC-3*$^{-/-}$ or *SRC-3*$^{+/+}$ littermate mouse embryos. When an adipogenic mixture was added, the accumulation of lipid droplets was completely blocked in *SRC-3*$^{-/-}$ compared with *SRC-3*$^{+/+}$ MEFs (Fig. 1*A*). The fact that a PPARγ ligand added in the adipogenic mixture is unable to bypass the deletion of *SRC-3* suggests that this coactivator could control either the gene expression of *PPARγ* and/or another PPARγ downstream event.

Considering that several genes are expressed specifically during adipogenesis and that the timing of the expression of these genes is essential for the acquisition and maintenance of the adipocyte phenotype, we examined the impact of the deletion of the *SRC-3* gene on the expression of adipocyte markers, using RT-PCR analysis of RNA isolated from MEFs before (day 0) and after complete adipocyte differentiation (day 12). Expression of genes including glucose transporter 4 (*Glut4*), adipocyte lipid-binding protein (*aP2/ALBP*), and *PPARγ* 2 were markedly decreased in *SRC-3*$^{-/-}$ MEFs (Fig. 1*B*).

To exclude any potential unspecific effect caused by the

Author contributions: J.-F.L. and A.C. contributed equally to this work. J.-F.L. and B.W.O. designed research; J.-F.L., A.C., L.A., and M.T.-L. performed research; R.-C.W. contributed new reagents/analytic tools; S.Y.T., M.-J.T., and J.A. analyzed data; and J.-F.L. and B.W.O. wrote the paper.

The authors declare no conflict of interest.

Abbreviations: C/EBP, CAAT/enhancer-binding protein; CBP, CREB-binding protein; MEF, mouse embryonic fibroblast; PPARγ, peroxisome proliferator-activated receptor; SRC-3, steroid receptor coactivator-3; WAT, white adipocyte tissue.

¶To whom correspondence should be addressed. E-mail: berto@bcm.tmc.edu.

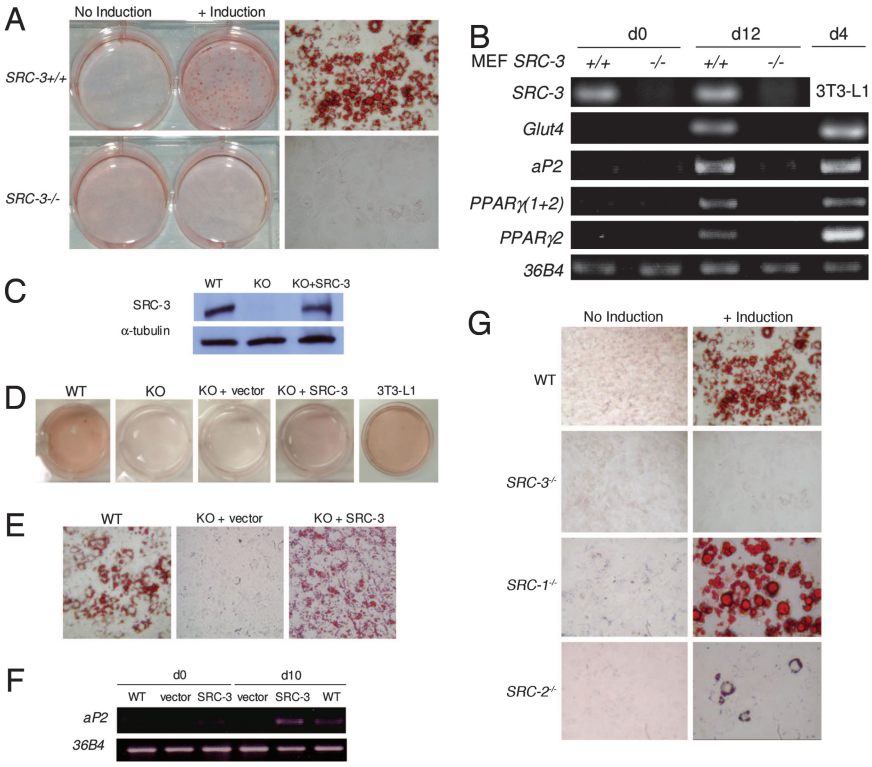

Fig. 1. Adipocyte differentiation is inhibited in *SRC-3*$^{-/-}$ MEF cells and the reexpression of SRC-3 in SRC-3 null cells restores adipogenesis. (*A*) Oil red O staining of WT and *SRC-3*$^{-/-}$ MEFs before induction of adipocyte differentiation (day 0) and after complete differentiation (day 12). (*Right*) Stained MEF cells. (Magnification: ×20.) (*B*) Expression of SRC-3 and adipogenic markers analyzed by RT-PCR in *SRC-3*$^{-/-}$ and WT MEFs. (*C*) Western blot analysis of SRC-3 protein levels in WT, *SRC-3*$^{-/-}$ (KO), and rescued *SRC-3*$^{-/-}$ (KO+SRC-3) MEF cells. α-tubulin served as a loading control. (*D*) Oil red O staining of WT, *SRC-3*$^{-/-}$ (KO), rescued *SRC-3*$^{-/-}$ (KO+SRC-3), and *SRC-3*$^{-/-}$ containing the empty vector (KO+vector) MEF cells. (*E*) Oil red O-stained WT, rescued *SRC-3*$^{-/-}$ (KO+SRC-3), and *SRC-3*$^{-/-}$ containing the empty vector (KO+vector) MEF cells. (Magnification: ×40.) (*F*) RT-PCR analysis of *aP2* gene expression in WT, rescued *SRC-3*$^{-/-}$ (SRC-3), and *SRC-3*$^{-/-}$ containing the empty vector (vector) MEF cells after adipocyte differentiation. *36B4* served as a loading control. (*G*) Oil red O staining comparing the induction of adipocyte differentiation of WT MEFs and knockout MEFs of each of the p160 coactivator family members.

immortalization of MEF cells, we rescued *SRC-3* gene expression in *SRC-3*$^{-/-}$ MEFs by using stable transfection of a vector expressing SRC-3 (Fig. 1*C*). The reexpression of SRC-3 in *SRC-3*$^{-/-}$ MEF cells led to the reactivation of the adipocyte-differentiation program as shown by the appearance of lipid droplets revealed by oil red O staining (Fig. 1 *D* and *E*). Consistently, the major adipocyte specific marker *aP2* was induced after addition of the adipogenic mixture in the rescued MEF cells as checked by RT-PCR (Fig. 1*F*). Taken together, the findings indicate that SRC-3 seems to play a cell-autonomous role in the adipocyte-differentiation process.

In concert with investigations of SRC-3, we studied the impact of the two other members of the p160 family on adipocyte differentiation. Interestingly, using the same protocol of MEF cell immortalization and differentiation, we found that of all of the SRC- null MEFs, *SRC-3*$^{-/-}$ MEFs present the most striking adipogenic phenotype (Fig. 1*G*). Indeed, the lack of SRC-1 had no detectable impact on lipid accumulation (Fig. 1*G*). Lipid droplet accumulation in *SRC-2*$^{-/-}$ MEFs was decreased compared with wild-type (WT) cells. This defect in triglyceride accumulation in the *SRC-2*$^{-/-}$ MEFs was, however, less pronounced than that observed in *SRC-3*$^{-/-}$ MEFs (Fig. 1*G*). Together, these results support a critical role for SRC-3 in the white adipocyte-differentiation program, and they suggest that the three members of the p160 coactivator family have nonredundant functions during adipogenesis.

SRC-3 Increases in the Nucleus During Early Stages of Adipocyte Differentiation, and It Accumulates to High Levels in the Nucleus of Differentiated Fat Cells. To determine the eventual dynamic role of SRC-3 occurring during the adipogenic program, we attempted to dissect the specific spatiotemporal relationships existing between SRC-3 protein and the subcellular context in which it functions. Using immunofluorescent staining of endogenous SRC-3 protein in intact 3T3-L1 cells during the course of adipogenesis, we observed a significant increase in SRC-3 protein levels in the nucleus in the early steps of fat-cell differentiation (Fig. 2*A*). This result was confirmed by quantitative analysis of nuclear fluorescence intensity (Fig. 2*B*) as well as by Western blotting (Fig. 2*C*). More interestingly, using high-resolution single-cell analysis, we have been able to determine a specific correlation between the differentiation status of 3T3-L1 fat cells and the protein levels of the coactivator SRC-3 in the nucleus (Fig. 2 *D* and *E*). Indeed, intense cytoplasmic staining of lipid droplets by the fluorescent dye Bodipy revealed that differentiated fat cells correlated with high SRC-3 protein levels in the nucleus. In contrast, cells with low levels of SRC-3 showed only a weak staining of triglycerides. Thus, these results are consistent with SRC-3 as a major player in the temporally controlled complex network of gene expression during fat-cell accumulation.

Transcriptional Impact of SRC-3 on *PPARγ2* Promoter. To dissect finely the specific molecular action of SRC-3 in adipocyte differentiation, we examined the impact of SRC-3 on a crucial checkpoint for the adipogenic program, that is, the control of expression of the *PPARγ2* gene (11, 12). During fat-cell differentiation, the expression of *PPARγ2* is subject to control by transcription factors such as C/EBP, the E2Fs, and Kruppel-like factor 5 (13–15). Based on these prior observations, we tested the transcriptional impact of SRC-3 on an artificial reporter plasmid containing multimerized C/EBP binding sites. SRC-3 stimulated the activity of this reporter synergistically with C/EBP in transient transfection experiments (Fig. 3*A*). We next examined whether SRC-3 coactivates *PPARγ2* transcription by using a reporter gene of the proximal promoter of the *PPARγ2* gene, containing several functional C/EBP-binding sites (13, 16). SRC-3 synergistically transactivated the *PPARγ2* promoter reporter in presence of C/EBPα or C/EBPδ (Fig. 3*E*). The impact of C/EBPβ was not analyzed in this work because its effect on *PPARγ2* proximal promoter is controversial (17). Importantly, the synergism of C/EBPα or δ and SRC-3 on *PPARγ2* promoter activity was significantly decreased by site-directed mutagenesis of the C/EBP-responsive elements (Fig. 3*B*).

SRC-3 Controls *PPARγ2* Gene Expression by Interacting with the Transcriptional Factor C/EBP on the Proximal Promoter. To confirm that the induction of the *PPARγ2* promoter by SRC-3 translated

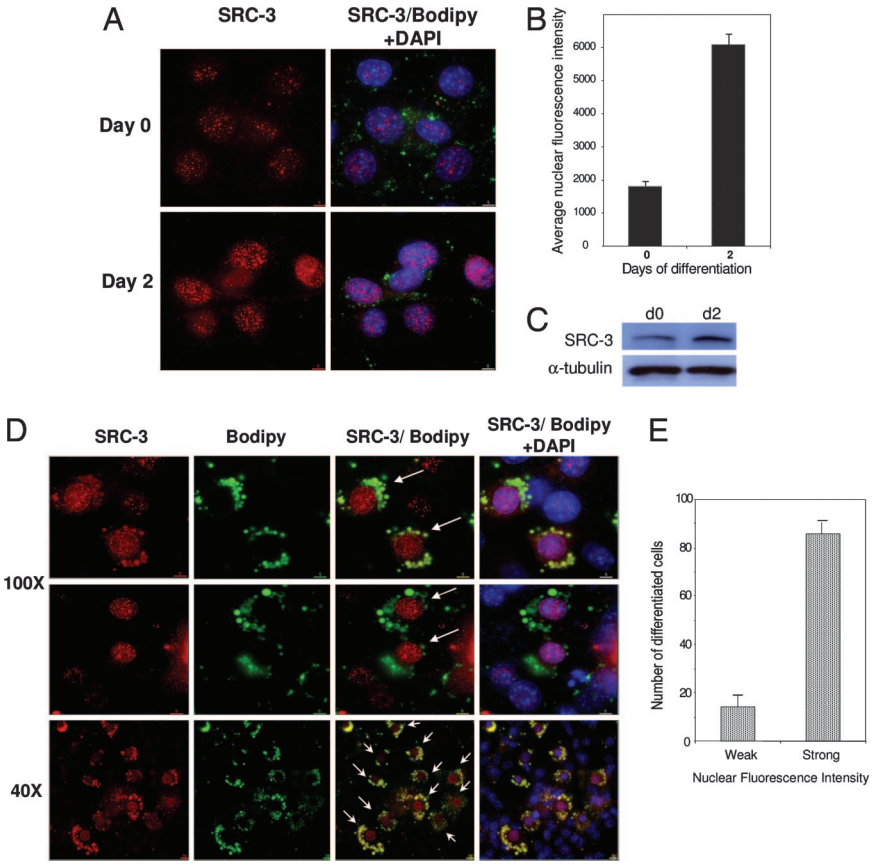

Fig. 2. Increased nuclear levels of SRC-3 in the early steps of adipocyte differentiation and accumulation to high levels in the nucleus of differentiated fat cells. (*A*) Immunofluorescence staining of SRC-3 protein in intact 3T3-L1 cells in the early steps of adipocyte differentiation. The fluorescent dye Bodipy and DAPI were, respectively, used to stain the lipids contained in the droplets of differentiated fat cells and nuclei of existing cells. (*B*) Quantitative analysis of nuclear fluorescence intensity in the early stages of 3T3-L1 fat-cell differentiation. (*C*) Western blot analysis of SRC-3 protein levels in 3T3-L1 differentiating cells in the early steps of adipocyte differentiation. α-tubulin served as a loading control. (*D*) Immunofluorescence staining of SRC-3 protein in intact 3T3-L1 cells in the late steps of adipocyte differentiation (day 4). [Magnification: $\times$100 (*Upper*); $\times$40 (*Lower*).] Arrows indicate that cells showing high SRC-3 protein levels in the nucleus have intense cytoplasmic staining of lipid droplets. (*E*) Quantification of differentiated 3T3-L1 fat cells showing strong nuclear localization of SRC-3. One hundred differentiated cells showing intense lipid droplet staining (size >2 μm) were counted manually for either strong (nuclear fluorescence value $>2 \times 10^3$) or weak nuclear SRC-3 fluorescence intensity (nuclear fluorescence value lower than 2×10^3). Errors bars represent S.E.M.

into increased *PPARγ2* mRNA levels, we monitored the expression of the endogenous *PPARγ2* gene during fat-cell differentiation of *SRC-3*$^{-/-}$ and *SRC-3*$^{+/+}$ MEFs. A strong and sustained expression of *PPARγ2* was observed in *SRC-3*$^{+/+}$ MEFs from day 8 of adipocyte differentiation onward; in contrast, *PPARγ2* mRNA levels were lower at day 8 in *SRC-3*$^{-/-}$ MEFs, and they became undetectable at day 12 (Fig. 4*A*).

To consolidate the molecular model in which SRC-3 transactivates *PPARγ2* in cooperation with specific transcriptional factors of the C/EBP family, coimmunoprecipitation assays were performed. In cultured cells, we were able to show a specific physical interaction between SRC-3 and C/EBPα or C/EBPδ (Fig. 4*B*). Moreover, chromatin samples were prepared from 3T3-L1 cells after induction of adipocyte differentiation and analyzed by ChIP assays using specific antibodies against C/EBPδ, C/EBPα, and SRC-3. No binding of these proteins to the *PPARγ2* promoter was observed on days 0 and 1 (Fig. 4*D*). At day 3 of differentiation, both C/EBPδ and SRC-3 are bound to the *PPARγ2* promoter, suggesting that the coactivator needs the presence of C/EBPδ at early steps of differentiation. By day 7, although C/EBPδ is not detected any more, SRC-3 is still present with C/EBPα, suggesting that SRC-3 is now recruited to the DNA through C/EBPα in the late steps of the differentiation process. No binding of C/EBP factors or SRC-3 was observed in a control region around $-1{,}500$ bp from the transcriptional start site of the *PPARγ2* gene, a region that does not contain a C/EBP-binding site (Fig. 4*D*). Collectively, these data suggest that the specific presence of SRC-3 in the chromatin context of the *PPARγ2* gene facilitates its expression.

To integrate SRC-3 into the cascade of the adipogenic program, we propose a scenario wherein SRC-3 interacts with C/EBPδ when expressed in the early steps of adipocyte differentiation and that this complex then controls *PPARγ2* gene expression (Fig. 4*E*). Thereafter, C/EBPα and other transcription factors bind to the *PPARγ2* promoter at the late steps of fat-cell differentiation, and SRC-3 continues to act through these "late" transcription factors to control *PPARγ2* expression (Fig. 4*E*).

***SRC-3*$^{-/-}$ Mice Show Reduced Fat Mass and a Significant Decrease of *PPARγ2* Gene Expression.** Finally, we attempted to validate our cellular observations by studying the *in vivo* impact of SRC-3 deletion on WAT biology. The tissue distribution of the SRC-3 gene expression in major metabolic tissues, explored by quantitative real-time PCR, clearly showed that SRC-3 was expressed at highest levels in the white adipose tissue compared with the other tested tissues, including the muscle and the liver (Fig. 5*A*). This observation suggested the existence of a biological relevance of this coactivator in this tissue. We then monitored weights of *SRC-3*$^{+/+}$ and *SRC-3*$^{-/-}$ mice. *SRC-3*$^{-/-}$ animals weighed less relative to their WT littermates (Fig. 5*B*). In addition, when the body-fat content was measured by dual-energy x-ray absorptiometry in *SRC-3*$^{+/+}$ and *SRC-3*$^{-/-}$ mice fed a chow diet, *SRC-3*$^{-/-}$ mice had a significantly lower total body-fat content than WT animals (Fig. 5*C*). These differences were mirrored by the reduced weight of the epididymal WAT depot in *SRC-3*$^{-/-}$ mice at death (Fig. 5 *D* and *E*). The decreases in body and fat weight occurred despite the fact that the *SRC-3* mutation did not affect food intake, absorption, and locomotor activity (data not shown). The reduction in adiposity was primarily the result of a significant reduction in adipocyte volume observed in *SRC-3*$^{-/-}$ mice compared with WT animals as assessed by classical hematoxylin/eosin staining (Fig. 5*F*), suggesting the existence of a defect in terminal adipocyte differentiation and fat accumulation.

The expression of major markers involved in the white-adipogenic program in mice was examined by quantitative real-time PCR. Importantly, the *PPARγ2* gene expression was

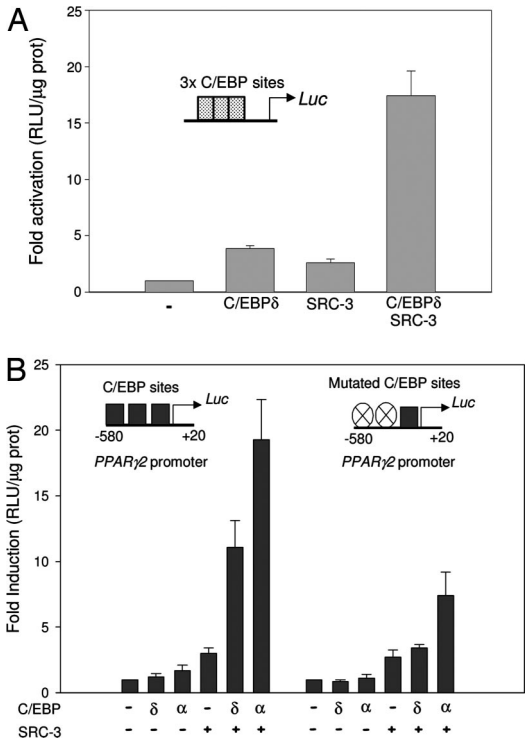

Fig. 3. Transcriptional effects of the coactivator SRC-3 on *PPARγ2* promoter. (*A*) Transient transfections experiments in HeLa cells testing the transcriptional impact of SRC-3 on an artificial promoter sequences containing a multimerized C/EBP binding sites. (*B*) Transient transfections using reporter constructs containing *PPARγ2* proximal promoter WT (*Left*) and mutated (*Right*) driving the expression of the luciferase (*Luc*) gene, in the presence or absence of expression vectors of SRC-3 and/or C/EBPα, and/or C/EBPδ. For each experiment, values represent means ± SEM of at least three independent experiments.

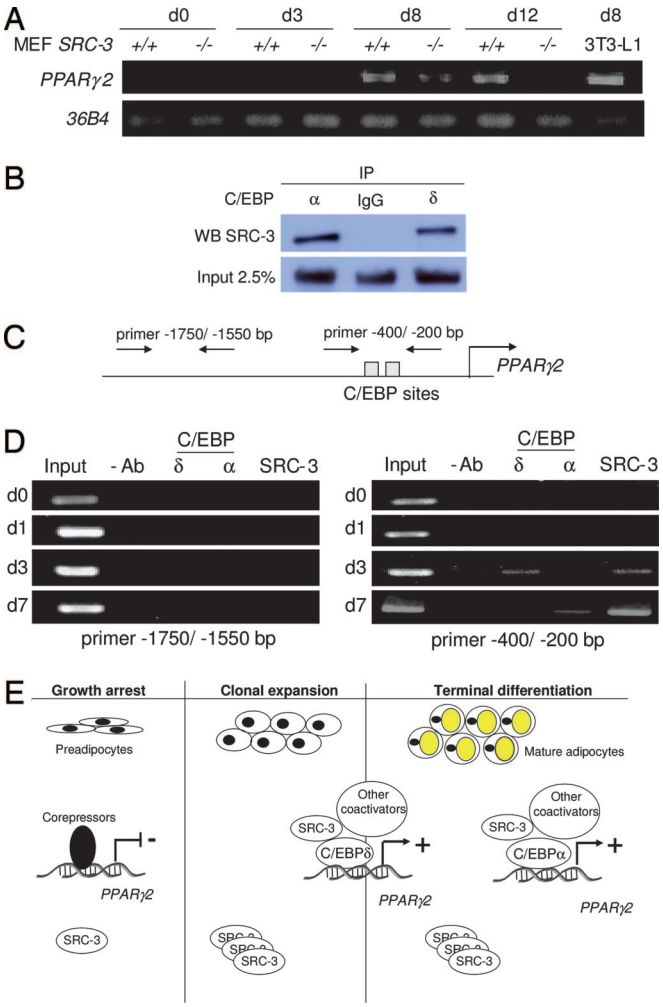

Fig. 4. SRC-3 transactivates the *PPARγ2* gene through a direct interaction with C/EBP on the PPARγ2 proximal promoter. (*A*) RT-PCR analysis of endogenous *PPARγ2* gene expression in MEFs from WT and SRC-3-null mice during the course of fat-cell differentiation. (*B*) Coimmunoprecipitation assays showing a physical interaction between SRC-3 and C/EBPα or C/EBPδ. (*C*) Schematic representation of the PPARγ2 proximal promoter showing the location of the primers used for ChIP assays. (*D*) ChIP analysis of SRC-3 and C/EBPs binding on *PPARγ2* proximal promoter. (*E*) Schematic representation of SRC-3 functions in adipocyte differentiation (see *Results*).

dramatically decreased, and it was found to be at undetectable levels in epididymal fat of *SRC-3*$^{-/-}$ animals compared with WT mice (Fig. 5*G*). This result is in clear consistency with our previous cellular observations. The adipogenic marker (*LPL*) gene, known as a target of PPARγ2 (18), also was significantly decreased. Moreover, *aP2* and *Glut4* were also decreased but only modestly (Fig. 5*G*). The persistence of the isoform PPARγ1 as well as the concomitant up-regulation of the transcription factor sterol-regulatory element-binding protein 1c may contribute to basal development of WAT in a PPARγ2-independent manner (Fig. 5*G*). These developmental and/or physiological adaptation events are still under investigation, and they could likely be influenced further by unknown coactivators.

Collectively, our *in vivo* observations that reveal a lean phenotype of SRC-3-null mice as well as a reduced gene expression of selective markers of adipogenesis, including the master regulator PPARγ2, highlight the important role played by the coactivator SRC-3 in WAT.

Discussion

Metabolic homeostasis is maintained by specific regulatory circuits controlled to a large extent by transcriptional mechanisms. The stepwise process of transcription involves many specialized proteins and coregulator complexes working together to express a given gene in a spatiotemporal manner (19–21). In the last few years, significant strides have been made in understanding the molecular mechanisms that regulate adipose tissue development and function, including the identification of multiple transcription factors (22, 23). However, the role of coregulators is still largely unexplored in adipose tissue biology.

In the present study, we demonstrate that the coactivator SRC-3 has a strong impact on the white adipocyte formation. In fact, the differentiation of the white adipocyte is completely inhibited in cultured cells in the absence of SRC-3. In addition to induction of SRC-3 in the early steps of adipocyte differentiation, a specific correlation exists between high nuclear levels of SRC-3 and highly differentiated fat cells. In an *in vivo* context where a variety of hormonal influences and tissue interrelationships exist, the WAT mass in *SRC-3*$^{-/-}$ mice is significantly reduced. Moreover, this reduction in adiposity is specifically associated with a dramatic decrease of PPARγ2 gene expression in the WAT of *SRC-3*$^{-/-}$ mice compared with WT animals. Whether PPARγ is univocally considered as the ultimate effector of adipogenesis, the relative contribution of the two PPARγ isoforms, PPARγ1 and 2, in this process is still a matter of debate. However, different convergent arguments suggest that PPARγ2 plays the dominant role. In fact, the nuclear receptor PPARγ2 is expressed almost exclusively in the

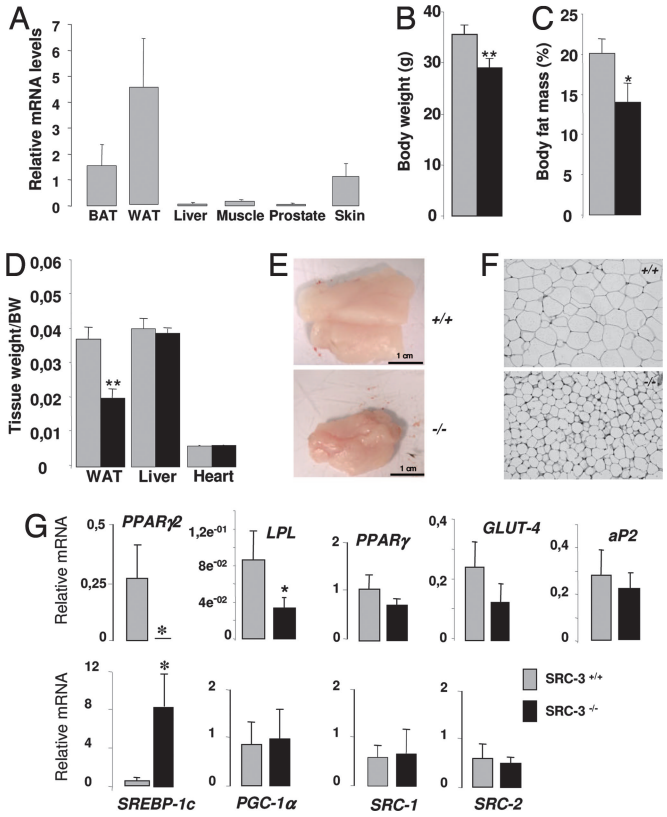

Fig. 5. *SRC-3*$^{-/-}$ mice present reduced adiposity and a significant decrease of gene expression of selective markers of adipogenesis including the master gene *PPARγ2*. (*A*) Analysis of *SRC-3* mRNA levels in metabolic tissues by real-time PCR. Tissue samples were extracted from WT mice ($n = 8$). (*B*) Body weight was evaluated in anesthetized 16-week-old male *SRC-3*$^{+/+}$ and *SRC-3*$^{-/-}$ mice ($n = 8$) fed a regular chow diet. (*C*) Body-fat mass was evaluated in anesthetized 16-week-old male *SRC-3*$^{+/+}$ and *SRC-3*$^{-/-}$ mice ($n = 8$) fed a regular chow diet by dual-energy x-ray absorptiometry. (*D*) Comparison of epididymal WAT, liver, and heart weights in *SRC-3*$^{+/+}$ and *SRC-3*$^{-/-}$ mice ($n = 8$) fed a regular chow diet. (*E*) Macroscopic images of *SRC-3*$^{+/+}$ and *SRC-3*$^{-/-}$ epididymal WAT. (*F*) Hematoxylin/eosin-stained WAT sections in *SRC-3*$^{+/+}$ and *SRC-3*$^{-/-}$ mice. (Magnification: ×10.) (*G*) mRNA levels of genes involved in adipogenesis in WAT of *SRC-3*$^{-/-}$ and *SRC-3*$^{+/+}$ mice ($n = 8$) determined by quantitative RT-PCR. Significance compared with *SRC-3*$^{+/+}$ mice: *, $P < 0.05$; and **, $P < 0.01$.

WAT tissue in contrast to PPARγ1, which is more widely expressed throughout the organism (e.g., adipose tissue, pancreatic B cells, macrophages, vascular endothelium) (3). In human, adipose expression of the PPARγ2 gene but not the PPARγ1 gene is increased in obese men and women, and the ratio of PPARγ2 to PPARγ1 is directly correlated with the body mass index (24). In addition, mice harboring a selective disruption of PPARγ2 expression showed a strong reduced level of the WAT mass (25). Finally, cellular studies using molecular tools to suppress specifically the expression of each PPARγ isoform in 3T3-L1 cells demonstrated that the level of PPARγ2 expression but not PPARγ1 correlated with the degree of lipid accumulation (26). Based on these multiple studies illustrating the crucial role that PPARγ2 plays in the white adipogenic program, our *in vivo* observations showing a significant decrease of PPARγ2 gene expression when SRC-3 is deleted, strongly reinforce the fact that SRC-3 is a key player in the integration of genetic events controlling the white adipogenic program.

The impact of SRC-3 on adipocyte differentiation can be explained by its ability to regulate directly or indirectly the transcriptional activity of genes coding for important mediators of adipogenesis. In this study, we provide evidence for direct control of the expression of the master gene of adipocyte differentiation *PPARγ2* by the coactivator SRC-3 through cooperative interactions with C/EBP family members. Interestingly, our study also provides an instance of a physical and functional interaction between a basic leucine zipper class of transcription factor and a SRC family coactivator. Prior publications have demonstrated that the expression of C/EBP family members is regulated during adipocyte differentiation. Indeed, MEF cells lacking both C/EBPβ and δ are severely impeded in their development as adipocytes (27). *C/EBPα*$^{-/-}$ mice have dramatically reduced fat accumulation in WAT pads apparently as a result of depressed lipogenesis because markers of fat-cell differentiation are expressed in the fat pads of these animals (28).

The characterization of animal models deficient in several different coregulators highlights an emerging and important role of this class of transcriptional modulators in vital metabolic processes linked to adipocyte differentiation. For instance, mice with a heterozygous deficiency in the coregulator CREB-binding protein (*CBP*) are lipodystrophic, and they are protected from diet-induced obesity (29). The phenotypic similarities between the *SRC-3*$^{-/-}$ and *CBP*$^{+/-}$ mice could in part be explained by the established fact that SRC-3 and CBP usually act in concert to regulate gene expression. These two factors have been purified in the same complex, and they have been implicated in numerous common physiological functions (30). In addition to CBP, the absence of TRAP220 impedes adipocyte differentiation, and *RIP140*$^{-/-}$ mice are lean (31, 32). These observations indicate the likely involvement of multiple multisubunit coregulator complexes in adipogenesis and energy homeostasis.

Collectively, our data highlight a pivotal role for the coactivator SRC-3 in white fat-cell differentiation by controlling major players in the genetic cascade that governs adipogenesis. Existing in large multisubunit coregulator complexes that provide enzyme activities that bridge nuclear receptors with the basal transcriptional machinery (21), SRC-3 itself can finely be regulated through posttranslational modifications such as selective phosphorylation (33, 34). Consequently, we suggest that SRC-3 represents one of the integrating links between the myriad of hormonal and/or metabolic signals known to influence adipogenesis (35) and the network of transcription factor complexes that control this process of differentiation.

Materials and Methods

Animal Experiments. The generation of the SRC-3$^{-/-}$ mice has been described in ref. 36. All mice were maintained on a pure C57BL/6J background. Only male, aged-matched (10–16 weeks old) mice were used. Animals were maintained in a temperature-controlled (23°C) facility with a 12-hr light/dark cycle. Mice had access to water and regular rodent chow (DO4; UAR, Villemoisson sur Orge, France). Body weight was recorded, and body fat mass was evaluated in anesthetized mice by dual-energy x-ray absorptiometry (PIXIMUS; GE Healthcare, Buc, France).

Histological Studies. Pieces of WAT from the mice were fixed in Bouin's solution, dehydrated in ethanol, embedded in paraffin, and cut at a thickness of 5 μm. Sections were deparaffinized, rehydrated, and stained with hematoxylin/eosin.

Cell Culture and Treatments. HeLa and 3T3-L1 cells were obtained from American Type Culture Collection (Manassas, VA), and MEF cells were prepared as described in ref. 33. 3T3-L1 and MEF cells were induced for differentiation by using standard protocols (37).

RNA Extraction and RT-PCR Analysis. RNA preparation was done by using the RNAeasy extraction kit (Qiagen, Valencia, CA). Classical RT-PCR was performed by using the two-step RT-PCR kit (Promega, Madison, WI) using the same amount of

mRNA for all samples. Quantitative RT-PCR was performed by using LightCycler FastStart DNA Master SYBR Green I from Roche Diagnostics (Pleasanton, CA) as specified. 18S rRNA was used as invariant control for the quantitative assays. The sequences of all used primers are available on request.

Plasmid Transfections and Luciferase Assays. C/EBPδ and C/EBPα cDNA inserted into pSV-SPORT1 expression vector were described in ref. 17. The luciferase reporter gene driven by a multimerized C/EBP element (3×C/EBP) was obtained from Stratagene (La Jolla, CA). PPARγ2 promoter (−580/+20) and the mutant cis-element constructs were described in ref. 13. HeLa cells were transfected at 70% of confluence, and luciferase activity was measured and normalized against total concentration of proteins. All transfection experiments were repeated at least three times in triplicate.

Immunocytochemistry and Quantitative Analysis of Fluorescence Intensity by High-Throughput Microscopy. 3T3-L1 cells were fixed with a solution of 4% formaldehyde before being exposed overnight to the rabbit anti-SRC-3 antibody (4°C) (30) and to secondary labeling with anti-rabbit Alexa Fluor 555 (Molecular Probes, Eugene, OR). Cells were counterstained with DAPI and Bodipy 493/503 (Molecular Probes). For details of quantitative analysis of fluorescence intensity by high-throughput microscopy, see *Supporting Methods*, which is published as supporting information on the PNAS web site.

Reexpression of SRC-3 in SRC-3$^{-/-}$ MEF Cells. SRC-3$^{-/-}$ MEF cells were cotransfected with either pTRE-tight-SRC-3 or the empty vector pTRE-tight, and pPuro and pTet-On (Clontech, Mountain View, CA). Forty-eight hours after transfection, cells were treated with trypsin, and stable transformants were selected with 0.25 μg/ml puromycin for 7–10 days. Pools of puromycin-resistant clones were screened for expression of SRC-3 by Western blotting after a 48-h induction with 1 mg/ml doxycycline. SRC-3 expressing clones were induced for adipocyte differentiation in presence of 1 mg/ml doxycycline following a standard protocol (37).

Coimmunoprecipitation Assays. HeLa cells were transiently transfected with either CMV-SRC-3 and pSV-SPORT1-C/EBPδ or pSV-SPORT1-C/EBPα or empty vectors. Then, HeLa cell lysates were incubated with anti- C/EBPα (Santa Cruz Biotechnology, Santa Cruz, CA) or anti-C/EBPδ (Santa Cruz Biotechnology) antibodies. The immune complexes were eluted and subjected to SDS/PAGE. The immunoblot detection was done by using anti-SRC-3 antibody (BD Biosciences, San Jose, CA).

ChIP Assays. ChIP analyses were performed by using an assay kit (Upstate Biotechnology, Lake Placid, NY) and anti-C/EBPδ (Santa Cruz Biotechnology), anti-C/EBPα (Santa Cruz Biotechnology), and anti-SRC-3 (BD Biosciences) antibodies. The sequences of all used primers are available on request.

Statistical Analysis. Data are presented as mean ± SEM. Statistical analyses were performed by using an unpaired Student's *t* test. Differences at $P < 0.05$ were considered to be statistically significant.

We thank Jiemin Wong and Michael Mancini for input and critical discussions and Maria Cristina Antal and Aurélie Auburtin from the Institut Clinique de la Souris for technical assistance. This work was supported by National Institutes of Health Grants 1-P01-DK59820-01 and HD07857 and by Centre National de la Recherche Scientifique, Institut National de la Santé et de la Recherche Médicale, Hôpitaux Universitaires de Strasbourg, and European Union Grant Eugene2 LSHM-CT-2004-512013.

1. Hausman DB, DiGirolamo M, Bartness TJ, Hausman GJ, Martin RJ (2001) *Obes Rev* 2:239–254.
2. Rosen ED, Walkey CJ, Puigserver P, Spiegelman BM (2000) *Genes Dev* 14:1293–1307.
3. Desvergne B, Wahli W (1999) *Endocr Rev* 20:649–688.
4. Tiraby C, Langin D (2003) *Trends Endocrinol Metab* 14:439–441.
5. Knouff C, Auwerx J (2004) *Endocr Rev* 25:899–918.
6. Anzick SL, Kononen J, Walker RL, Azorsa DO, Tanner MM, Guan XY, Sauter G, Kallioniemi OP, Trent JM, Meltzer PS (1997) *Science* 277:965–968.
7. Liao L, Kuang SQ, Yuan Y, Gonzalez SM, O'Malley BW, Xu J (2002) *J Steroid Biochem Mol Biol* 83:3–14.
8. Torres-Arzayus MI, De Mora JF, Yuan J, Vazquez F, Bronson R, Rue M, Sellers WR, Brown M (2004) *Cancer Cell* 6:263–274.
9. Coste A, Antal MC, Chan S, Kastner P, Mark M, O'Malley BW, Auwerx J (2006) *EMBO J* 25:2453–2464.
10. O'Malley BW (2006) *Science* 313:1749–1750.
11. Camp HS, Ren D, Leff T (2002) *Trends Mol Med* 8:442–447.
12. Picard F, Auwerx J (2002) *Annu Rev Nutr* 22:167–197.
13. Clarke SL, Robinson CE, Gimble JM (1997) *Biochem Biophys Res Commun* 240:99–103.
14. Fajas L, Landsberg RL, Huss-Garcia Y, Sardet C, Lees JA, Auwerx J (2002) *Dev Cell* 3:39–49.
15. Oishi Y, Manabe I, Tobe K, Tsushima K, Shindo T, Fujiu K, Nishimura G, Maemura K, Yamauchi T, Kubota N, *et al*. (2005) *Cell Metab* 1:27–39.
16. Saladin R, Fajas L, Dana S, Halvorsen YD, Auwerx J, Briggs M (1999) *Cell Growth Differ* 10:43–48.
17. Elberg G, Gimble JM, Tsai SY (2000) *J Biol Chem* 275:27815–27822.
18. Schoonjans K, Peinado-Onsurbe J, Lefebvre AM, Heyman RA, Briggs M, Deeb S, Staels B, Auwerx J (1996) *EMBO J* 15:5336–5348.
19. Spiegelman BM, Heinrich R (2004) *Cell* 119:157–167.
20. Lonard DM, O'Malley BW (2006) *Cell* 125:411–414.
21. Rosenfeld MG, Lunyak VV, Glass CK (2006) *Genes Dev* 20:1405–1428.
22. Feve B (2005) *Best Pract Res Clin Endocrinol Metab* 19:483–499.
23. Rosen ED (2005) *Prostaglandins Leukotrienes Essent Fatty Acids* 73:31–34.
24. Vidal-Puig AJ, Considine RV, Jimenez-Linan M, Werman A, Pories WJ, Caro JF, Flier JS (1997) *J Clin Invest* 99:2416–2422.
25. Zhang J, Fu M, Cui T, Xiong C, Xu K, Zhong W, Xiao Y, Floyd D, Liang J, Li E, *et al*. (2004) *Proc Natl Acad Sci USA* 101:10703–10708.
26. Ren D, Collingwood TN, Rebar EJ, Wolffe AP, Camp HS (2002) *Genes Dev* 16:27–32.
27. Tanaka T, Yoshida N, Kishimoto T, Akira S (1997) *EMBO J* 16:7432–7443.
28. Wang ND, Finegold MJ, Bradley A, Ou CN, Abdelsayed SV, Wilde MD, Taylor LR, Wilson DR, Darlington GJ (1995) *Science* 269:1108–1112.
29. Yamauchi T, Oike Y, Kamon J, Waki H, Komeda K, Tsuchida A, Date Y, Li MX, Miki H, Akanuma Y, *et al*. (2002) *Nat Genet* 30:221–226.
30. Wu RC, Qin J, Hashimoto Y, Wong J, Xu J, Tsai SY, Tsai MJ, O'Malley BW (2002) *Mol Cell Biol* 22:3549–3561.
31. Ge K, Guermah M, Yuan CX, Ito M, Wallberg AE, Spiegelman BM, Roeder RG (2002) *Nature* 417:563–567.
32. Leonardsson G, Steel JH, Christian M, Pocock V, Milligan S, Bell J, So PW, Medina-Gomez G, Vidal-Puig A, White R, Parker MG (2004) *Proc Natl Acad Sci USA* 101:8437–8442.
33. Wu RC, Qin J, Yi P, Wong J, Tsai SY, Tsai MJ, O'Malley BW (2004) *Mol Cell* 15:937–949.
34. Wu RC, Smith CL, O'Malley BW (2005) *Endocr Rev* 26:393–399.
35. Gregoire FM, Smas CM, Sul HS (1998) *Physiol Rev* 78:783–809.
36. Xu J, Liao L, Ning G, Yoshida-Komiya H, Deng C, O'Malley BW (2000) *Proc Natl Acad Sci USA* 97:6379–6384.
37. Picard F, Gehin M, Annicotte J, Rocchi S, Champy MF, O'Malley BW, Chambon P, Auwerx J (2002) *Cell* 111:931–941.